*Bull. Nov. Comp. Center*, Math. Model. in Geoph., 11 (2006), 85–92


# Mathematical modeling and experimental investigations of complex geological structures (using the mud volcano Shugo as an example)

B.M. Glinsky, M.S. Khairetdinov, A.G. Fatyanov

**Abstract.** Now about 700 volcanoes are believed to be active in the world. In this paper, both theoretical and experimental grounds of the monitoring system of living volcanoes with the use of powerful vibroseismic sources are considered. A method to calculate Green's function for inhomogeneous models of media with employment of the reciprocity principle was developed for the numerical modeling of arbitrary structures, in particular, magma chambers. A medium is assumed to consist of arbitrary blocks. A certain part of the medium can be a layered pack with an arbitrary number of layers. The thickness of layers and the velocity parameters of media can be arbitrary quantities in both the layered pack and in the block medium. It should be noted that the calculation of Green's function allows simultaneous calculation of the wave fields for an arbitrary number of sources and receivers. This is also important for problems of the 3D (areal) seismic prospecting and for solving inverse problems of geophysics by using optimization methods.

## Introduction

A vibroseismic sounding method with the use of powerful controllable sources with an action onto the ground of 40–100 tons was developed on the basis of mathematical modeling. The results of the first experimental works for the Taman mud volcano province are presented. The medium model in the mud volcano Shugo region obtained on the basis of vibroseismic sounding data was refined with the help of the numerical modeling.

In its activity, the volcano Shugo crater differs from the mud volcanoes of Taman and the North-West of Caucasia. It looks like a huge bowl, with a volcanic construction of light-gray breccia in the center. The bowl itself resembles a subsidence caldera. This distinguishes the volcano Shugo from other mud volcanoes of Taman and the North-West of Caucasia. Therefore, the volcano is most interesting not only from a geological, but also from a seismic standpoint. This substantiated the choice of an object to test the technology proposed for the monitoring of complex geological objects [1].

## 1. Mathematical modeling

The modeling of wave fields for an arbitrary location of the vibrator, recording systems, and parameters was made to justify experimental works in the

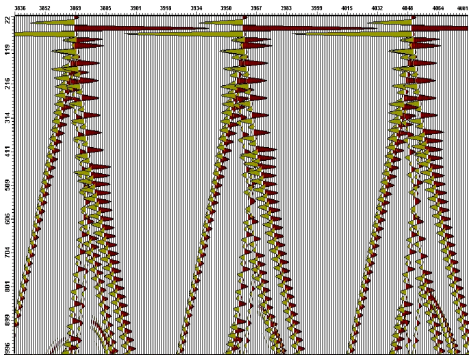

**Figure 1.** A fragment of a seismic profile in the presence of a volcanic zone

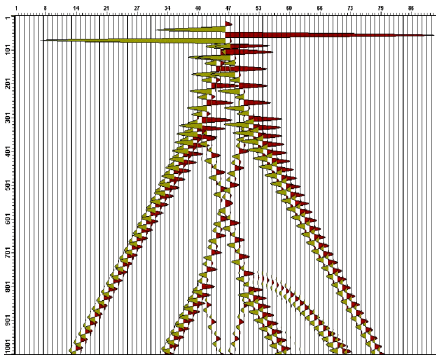

**Figure 2.** A seismogram with a source over the origin zone center

Taman mud volcano province [2]. As noted in [3], one can with sufficient confidence predict a fracture in the syncline core, that is an approach channel for the volcano Shugo. The mud volcano chamber is located just in the syncline, and the volcano "magmatic" origin is at a large depth. To determine the main peculiarities of the wave field for this region, the simulation was performed in several steps. First, for comparison, a simplified model of a rectangular fault without a volcanic chamber was taken. Then a volcanic chamber was introduced into the model. Figure 1 shows a fragment of a theoretical seismic profile for the Shugo volcano origin zone. A seismogram with a source in the origin zone center is presented in Figure 2.

## 2. Experimental results

From a methodological standpoint, the seismic sounding of the volcano involved a study of the transformation conditions of wave fields on geological structures as longitudinal profiles passed by the traverses "vibrator — recording seismic station — mud volcano" and "vibrator — volcano — recording seismic station". The scheme of sounding is presented in Figure 3.

In the adopted technology of field works, a geological structure was sounded by moving the seismic vibrator along the shown traverses and by arranging seismic sensors within the "source-receiver" base within 500–5500 m. The number of repeated sounding sessions at each vibrator installation point varied from 5 to 7, which was sufficient for increasing the noise immunity of vibrational seismograms in the case of increased seismic noise in the volcano region in the course of processing. Vibrational seismograms $\bar{r}(m)$ which are analogs of explosion seismograms, were calculated using the algorithm

$$\bar{r}(m) = \frac{1}{L}\sum_{i=1}^{L}\sum_{n=0}^{N-1} x_n^{(i)} S_{n-m}, \qquad m = 0, \ldots, M, \quad i = 1, \ldots, L. \tag{1}$$

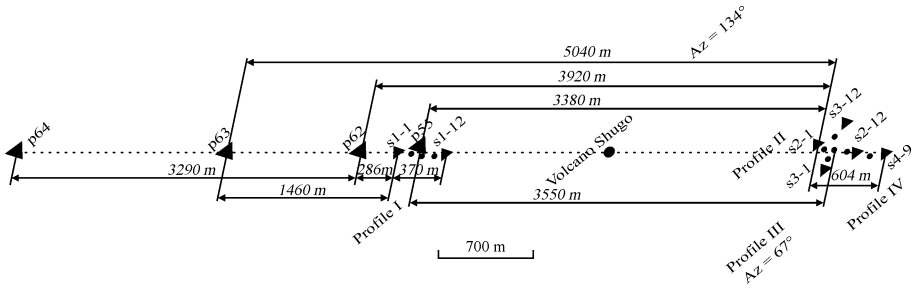


**Figure 3.** A scheme of installing the vibrator and sensors for vibrational sounding of the volcano Shugo: p55, p62, p63, p64 are sounding points, s1-1, s1-12, ... are seismic arrays, profiles I–IV are lines of arranging seismic arrays

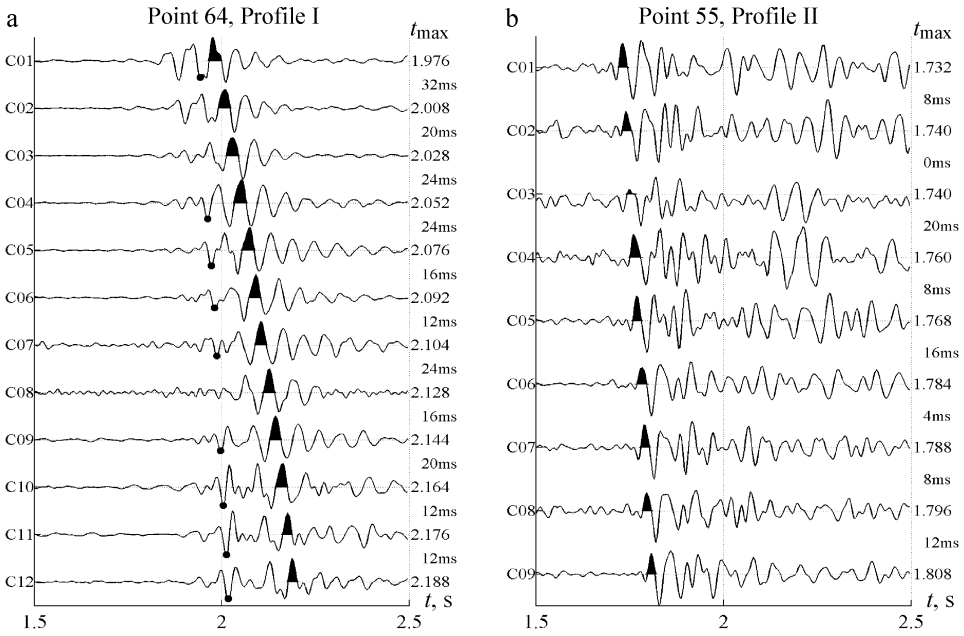


**Figure 4.** Vibrational seismograms obtained at profiles I (a) and II (b)

Here $M$ is the number of discrete samples of the vibrational seismogram, $L$ is the number of averaging, $S(t_n)$ is the reference signal with linear frequency modulation (LFM) of the form $S(t) = a(t)\cos(2\pi f_0 t + \beta t^2/2)$, whose parameters are $a(t)$, the envelope, $f_0$, the initial frequency of sweep, $\beta$ is the frequency sweep rate $\beta = (f_{\max} - f_0)/T$, where $f_{\max}$ is a maximum frequency and $T$ is the sweep duration.

In the experiment, the following quantities were taken as a basis: $f_0 = 10$ Hz, $f_{\max} = 64$ Hz, and $T = 60$ s. In this case, particular forms of vibrational seismograms $\bar{r}(m)$ obtained are presented in Figure 4.

The vibrational seismograms obtained in the experiments are characterized by a high ratio between the levels of useful waves and noise, which is about 20 in some cases. One can see that the character of seismograms abruptly changes when seismic waves are passing through a mud volcano zone.

Another important characteristic of the vibroseismic signals spectra is spectral-time functions (STF), which make it possible to study typical temporal peculiarities of the spectra of vibrational signals and obtained seismograms. It is significant that these processes are nonstationary and, hence, the spectral functions that describe them can be represented by an expression of the form $F(\omega, t)$. In this case, the algorithm to calculate the STF has the following form:

$$F(\omega_k, t_q) = F(k, q) = \sum_{n=0}^{N_1-1} x_{n+q} \exp\Big(-i\frac{2\pi kn}{N}\Big), \tag{2}$$

where $n = 0, 1, \ldots, N_1 - 1$, $q = 0, 1, \ldots, N_2 - 1$, $N_1 N_2 = N$, $N = T/\Delta t$, $T$ is the total time of analysis, and $\Delta t$ is a quantization interval of the initial signals.

As the sequences $x_{n+q}$, the initial signals recorded in the direction of an inlet of the recording system of seismic signals were used in one case, and the vibrational seismograms $\bar{r}(m)$ in the other case. The forms of these functions for both signals are presented in Figures 5 and 6.

With the technology adopted for the full-scale experiment, it was possible to do the following:

- fix peculiarities of wave structures in the vicinity of the volcanic construction and estimate a contribution of the induced waves to the parameters of recorded seismic fields;
- construct a velocity profile of a geological structure in the zone of the volcanic construction of the mud volcano Shugo.

Let us point out some most characteristic peculiarities of the recorded seismic fields. Vibroseismic sounding of the mud volcano body reveals a more complex field structure (see Figure 4b). This is due to the passage of seismic oscillations through a complex geological structure of the volcanic construction in comparison to the pattern of wave processes recorded in seismograms in front of the volcano (see Figure 4a). In the time domain, this leads to appearance in the vibrational seismograms of chaotically arranged (scattered) secondary waves arising after head waves (Figure 5b). In this case, the duration of a greater part of seismograms increases to 1.5–2 s instead of 0.3 s obtained in the first case. In all the appropriate STFs, an extension of the spectra of the medium responses (for instance, in Figure 6b)

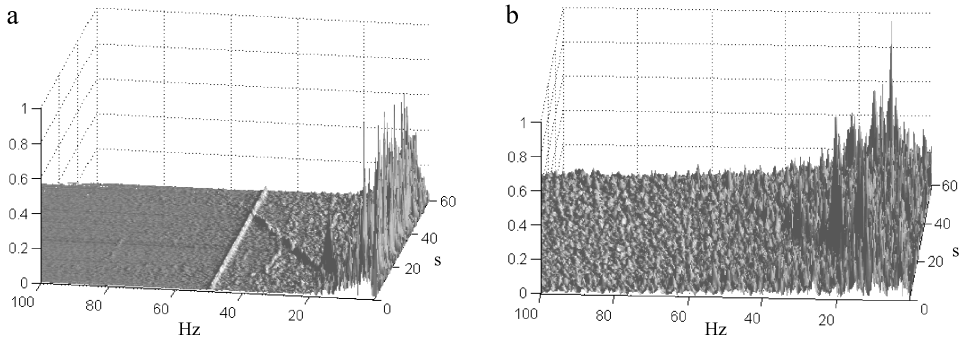


**Figure 5.** Spectral-time functions of the initial seismic signals for "vibrator–receiver" distances: a) $R = 3500$ m (in front of Shugo); b) $R = 3600$ m (behind Shugo)

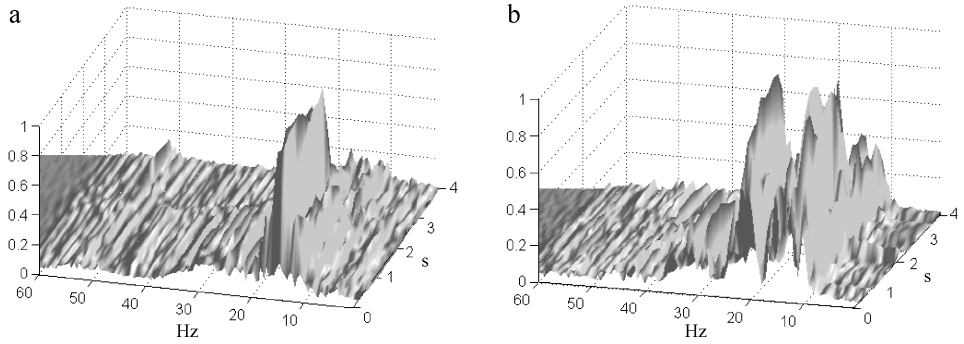


**Figure 6.** Spectral-time functions of vibrational seismograms for "vibrator–receiver" distances: a) $R = 3500$ m (in front of Shugo); b) $R = 3600$ m (behind Shugo)

in the sounding frequency range from 10 to 64 Hz in comparison with the narrowband responses (Figure 6a) recorded in front of the volcano at a distance of 550–3500 m is simultaneously observed. A comparison of the two STFs obtained "in front of the volcano" and "behind the volcano" at comparable "source-receiver" distances (see Figure 6a for 3500 m and Figure 6b for 3600 m) clearly shows the contribution of fluid-magmatic structures of the volcanic construction to the process the oscillation spectrum enrichment. In this case, a tenfold extension of the oscillation spectrum is observed.

Such effects can be related to the transformation of radiated signals on nonlinear structures of a geological structure when propagate seismic waves in fluid-saturated formations, such as effluent channels of mud volcanoes. It is important to mention the following features.

An additional feature of the seismic wave field at the volcano outlet is associated with the appearance of some resonances in characteristic frequency bands (see, for instance, Figure 6b, where two resonances are distinguished).

This is due to the presence of clearly defined structures with inherent resonant features (effluent channels, a mud volcanic chamber, etc.) inside the volcanic construction.

The STF maxima that characterize the resonant properties of the "radiator — wave propagation medium" scheme depend on a distance $R$ and, hence, lie within 40–50 Hz at $R = 550$ m, 20–30 Hz at $R = 1700$ m, and 15–20 Hz at $R = 3500$ m (see Figure 6a). Thus, the resonance is shifted to the lower frequencies domain as a distance increases.

At small distances from the source ($R = 550$ m) multiple (2nd, 3rd, and 4th) harmonics show up in the seismic wave field. As a distance increases, the harmonics weaken as a result of attenuation and, from a distance of 1700 m and longer, they do not manifest themselves.

The dominant level of noise in the low frequencies domain (below 10 Hz) is observed in the initial signals STFs. From a comparison of the STFs of the initial vibroseismic signals (see Figure 5) and vibrational seismograms (see Figure 6), one can see a high selectivity of correlation convolution (1), which allows effective identification of a useful sweep signal on the noise background. This explains the absence of noise in the domain of low frequencies (below 10 Hz) in the STF plots presented in Figures 6a and 6b, in contrast to similar plots obtained for initial signals (see Figures 5a and 5b).

The reduced travel time curves of head seismic waves (reduction rate $V = 4550$ m/s) obtained by using the data of vibrational sounding have clear linear "time–distance" dependencies within 300–5000 m (Figure 7). An apparent average velocity of 1740 m/s corresponds to travel time curve I obtained at the "vibrator — receiver — volcano" profile. This velocity is repeated, with an accuracy of 0.5 %, in different sounding sections. An appar-

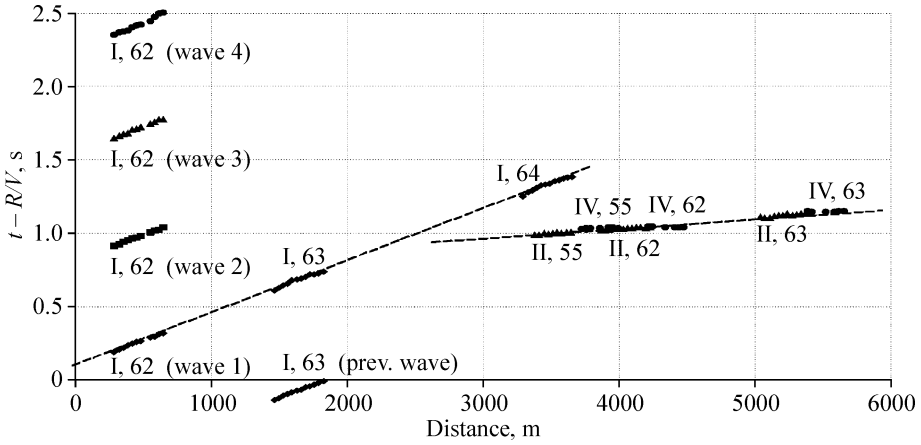


**Figure 7.** Reduced hodographs of waves for profiles I, II, and IV and sounding points 55, 62, 63, and 64

ent average velocity of 3400 m/s corresponds to the second travel time curve for profiles II and IV that fits the "vibrator — volcano — receiver" arrangement scheme (that is, the volcano is between the source and the receiver) with an accuracy of up to 3 %. Both hodographs were obtained by using vibrational seismograms with prominent arrivals of head waves.

As an example, Figure 4a shows vibrational seismograms, in which waves are for both the first travel time curve (with blackened positive phases) and the second travel time curve (with waves denoted by dots). Figure 4b shows the head waves corresponding to the second travel time curve. These data are obtained for the Shugo region and a vibrational sounding range of up to 5000 m and make it possible to adopt a model of three-layered horizontal medium, whose boundaries are at depths of 70 m and 702 m.

The data for the seismic profile, obtained on the basis of sounding by the method of reflected waves, along the Rostov–Novorossiisk line completed in 2000 by the GEON Center were used when constructing the cross-section deep part [4]. The data of vibroseismic exploration (VSE) allow adopting the model of three-layered horizontal medium with wave velocities $V_1$, $V_2$, $V_3$ and boundaries $H_1$, $H_2$ (Figure 8).

| |
|---|
| $V_1 = 1130$ m/s, $\quad H_1 = 70$ m |
| $V_2 = 1740$ m/s, $\quad H_2 = 632$ m |
| $V_3 = 3400$ m/s |

**Figure 8.** Three-layered model of the medium in the Shugo region

Numerical experiments have shown that the data of numerical calculations and real vibrograms for the model in Figure 8 considerably differ. In this case, the qualitative coincidence of theoretical and real vibrograms can be achieved by choosing the velocity in the half-space $V_3 = 4000$ m/s (Figure 9).

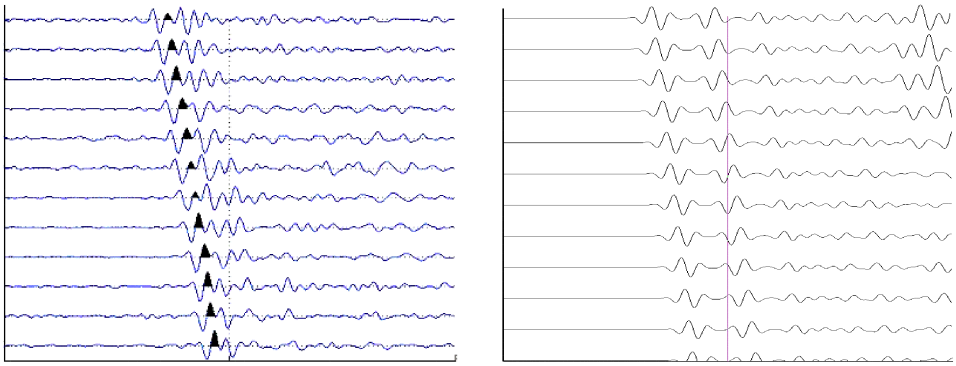

**Figure 9.** Experimental (left) and theoretical (right) vibrograms for the volcano Shugo. Sensor-source distance 3920 m

Geodynamic effects associated with the response of mud-effluent channels and other fluid-saturated structures in the volcanic construction body to the vibrational action were detected with active monitoring of the volcanic construction and a surrounding geological structure. The eruption of mud in the volcano center and at the periphery with long-lasting active seismic action display a spatial anisotropy.

In conducting the works, a temporary redistribution of mud eruption took place in all gryphons of the Shugo volcano. Some lateral gryphons began to erupt. Additional special experiments on mud volcanoes are needed to study this phenomenon. This is important because such processes seem to be indicators to preparation of the regional-scale seismic events. There is good reason to believe that the main reason for these anomalous geophysical phenomena can be the dynamic restructuring of dilatant structures of the resonant type, which develops in the volcanic construction body at all stages of its functioning.

## Conclusion

Active sounding of a volcanic construction, with the mud volcano Shugo (the Taman mud-volcanic province) as an example, was performed for the first time as a practical application of methods for vibroseismic monitoring of complex geological formations being developed in Russia. During the field experiments, a seismic cross-section in the volcano zone has been made, and the conditions of interaction of vibroseismic fields with a volcanic construction body and the surrounding geological structure have been studied. The observed structural changes of the dynamic characteristics of wave fields make it possible to analyze the conditions of generation of induced wave processes in the volcanic construction body at a new level. These experiments serve as basis for the creation of a system and methodology of active monitoring of living volcanoes with the use of vibrational sources.

## References

[1] Alekseev A.S., Glinsky B.M., Khairetdinov M.S., et al. New geotechnologies and complex geophysical methods of studying the interior structure and dynamics of geosphere / Ed. N.P. Laverov. — Moscow, 2002.

[2] Fatyanov A.G. Mathematical simulation of wave fields in media with arbitrary curvilinear boundaries // Appl. Math. Letters. — 2005. — Vol. 18, Iss. 11. — P. 1216–1223.

[3] Laverov N.P., Bogatikov O.A., Gurbanov A.G., et al. Geodynamics, Seismotectonics and Volcanos of Central Caucuses // Global Changes of an Environment and a Climate. — Moscow: Nauka, 1977. — P. 109–130.

[4] Zolotov et al. New data about a deep structure of an earth's crust and seismicity of the Western Caucasus // Geophysics XXI Century. — Moscow: Nauka, 2001. – P. 85–89.